Rev. Adv. Mater. Sci. 37 (2014) 90-96

NANODISTURBANCE DEFORMATION MODE IN FCC NANOWIRES, MICROPILLARS, AND BULK NANOCOMPOSITES

S.V. Bobylev[1,2,3] and I.A. Ovid'ko[1,2,3]

[1]Department of Mathematics and Mechanics, St. Petersburg State University, Universitetskii pr. 28, Staryi Peterhof, St. Petersburg 198504, Russia
[2]Institute of Problems of Mechanical Engineering, Russian Academy of Sciences, Bolshoj 61, Vasil. Ostrov, St. Petersburg 199178, Russia
[3]Research Laboratory for Mechanics of New Nanomaterials, St. Petersburg State Polytechnical University, St. Petersburg 195251, Russia

Received: January 10, 2014

Abstract. Nanodisturbance deformation mode in free-standing nanowires, micropillars and nanowires serving as structural elements of bulk nanocomposites is theoretically described for various metallic and covalent materials having face-centered cubic crystal lattices. This deformation mode represents formation of near-surface nanodisturbances, nanoscopic areas of ideal plastic shear with tiny shear vectors in subsurface areas of nanowires and micropillars. The critical stress is calculated which is needed for the nanodisturbance deformation mode to occur in nanowires/micropillars having square cross sections. This stress is calculated as a function of the nanowire/micropillar cross section size *d* ranging from 1 to 500 nm in the cases of metals (Al, Au, Ni, Pd) and covalent materials (Si, SiC). Sensitivity of the nanodisturbance deformation mode to geometric and material parameters of nanowires and micropillars is discussed.

1. INTRODUCTION

Unique mechanical and physical properties of nanowires and micropillars strongly depend on evolution of their defect structures which thereby represent the subject of intensive research in physics and materials science; see, e.g., [1–21]. Of particular interest are generation and evolution of defects carrying plastic flow in nanowires and micropillars exhibiting specific deformation behaviors and a dramatic increase in strength with reduction of nanowire/micropillar diameter [4–20]. For instance, metallic micropillars with diameters of around 200–500 nm under compression show superior strength with values exceeding by 10–50 times those of bulk metallic materials; see experiments [4,6,7,9,10,12-15,18]. This extraordinary high strength (which is close to the theoretical strength) is attributed to dislocation-free states of micropillars [6,7]. More precisely, following Greer and Nix [6,7], pre-existent dislocations under applied stress move towards micropillar free surfaces where they rapidly disappear. As a result of the fast initial deformation stage, a micropillar becomes free from dislocations, basic carriers of plastic flow in crystals. The further plastic deformation can occur, if only very high stresses are applied which initiate plastic flow in the defect-free micropillar [6,7].

Also, as with micropillars, ultrathin free-standing nanowires exhibit superior strength and are deformed by specific deformation modes [1,5,11,16,17]. In general, following experimental data, computer simulations and theoretical models in this area, one can distinguish several deformation modes operating in initially defect-free nanowires

Corresponding author: I.A. Ovid'ko; e-mail: ovidko@nano.ipme.ru

and micropillars at very high level of stresses. For instance, computer models [22,23] showed that plastic flow in initially defect-free nanowires occurs through nucleation of lattice dislocations at nanowire free surfaces and their further glide in nanowire interiors. Also, following experimental data [13], computer simulations [24] and theoretical models [17,25], nanoscale deformation twinning can come into play in nanowires and micropillars. Besides, solid state amorphization of initially crystalline and defect-free nanowires under mechanical load has been observed in experiment [26] and computer simulations [27,28]. These results are logically explained in the theoretical model [29] describing a nanoscale amorphization process associated with spatially inhomogeneous shear as a special mode of plastic deformation in nanowires. In addition, in papers [11,25] a new mechanism of plastic deformation in defect-free nanowires has been suggested and theoretically described. This mechanism represents the nanodisturbance deformation mode, that is, formation of near-surface nanodisturbances – nanoscopic areas of ideal plastic shear with tiny shear vectors – in single crystalline nanowires under mechanical load. It was theoretically demonstrated that, as with nanowires [11,25], Gum metals (special Ti-based alloys) [30], nanocrystalline materials [31,32] and nanocomposites [33] can be deformed by the nanodisturbance mechanism. These theoretical representations were confirmed by "in situ" observation (by high resolution electron microscopy) of nanodisturbances – carriers of nanoscale ideal shear – in Gum metals during their plastic deformation [34]. Also, nanoscale stacking faults resulting from nanoscale ideal shear events were experimentally observed in deformed Au nanowires with lateral sizes ≈1-2 nm [16]. Besides, Oh with co-workers [10] noted that nanodisturbances can produce dislocation loops experimentally observed in mechanically loaded micropillars.

In papers [11,25], operation of the nanodisturbance deformation mode in Au and Cu nanowires having square cross sections with sizes (analogs of diameters of cylinder-like nanowires) ranging from 1 to 50 nm was theoretically analyzed. The nanowires are made of metals (Au and Cu) specified by rather low values of the stacking fault energy, and the examined range (1 – 50 nm) of nanowire sizes is, in fact, limited to the cases of thin and ultrathin nanowires. At the same time, it is highly interesting to understand, if the nanodisturbance deformation mode can also operate in both nanowires and micropillars (with cross section sizes having values up to 500 nm) made of materials with covalent chemical bonding and metals with comparatively large values of the stacking fault energy. The main aim of this paper is to theoretically examine the energy and stress characteristics of the nanodisturbance deformation mode in both nanowires and micropillars made of such covalent materials as SiC and Si as well as various metals such as Al, Au, Ni, and Pd in the range of nanowire/micropillar cross section size from 1 to 500 nm. This examination will allow us to reveal fundamentally and practically important trends of sensitivity exhibited by the nanodisturbance deformation mode to geometric and material parameters of nanowires and micropillars.

2. GEOMETRIC FEATURES OF NANODISTURBANCE DEFORMATION MODE IN NANOWIRES, MICROPILLARS AND BULK NANOCOMPOSITES CONTAINING NANOWIRES

Let us consider the specific geometric features of the nanodisturbance deformation mode in a single crystalline nanowire/micropillar which is initially free from defects. For definiteness, we describe these geometric features in the exemplary case of a free-standing nanowire having initial shape of a long rectangular box with a square cross section having the sizes $d \times d$ (Fig. 1a). Results of our examination can be almost directly (with evident minor modifications) extended to nanowires and micropillars having other geometries (e.g., cylinder-like nanowires, micropillars growing on substrates, etc.).

So, let us consider the nanodisturbance deformation mode, that is, plastic flow occurring in a nanowire through formation of near-surface nanodisturbances, nanoscopic areas of plastic shear with tiny shear vectors formed near nanowire free surfaces (Fig. 1). At the initial stage of the nanodisturbance deformation mode, an applied shear stress causes a 'momentary' ideal (rigid-body) shear to occur along the nanoscale fragment ABCD of a nanowire section misoriented by 45 degrees relative to the nanowire axis (Fig. 1b). The shear is specified by a tiny shear magnitude s and produces a generalized stacking fault ABCD having nanoscopic sizes (Fig. 1b). (A generalized stacking fault is by definition a planar defect resulted from a cut of a perfect crystal across a single plane into two parts which are then subjected to a relative displacement through an arbitrary vector **s** (lying in the cut plane) and rejoined; see, e.g., [35,36].) The generalized stacking fault is bounded in the nanowire section

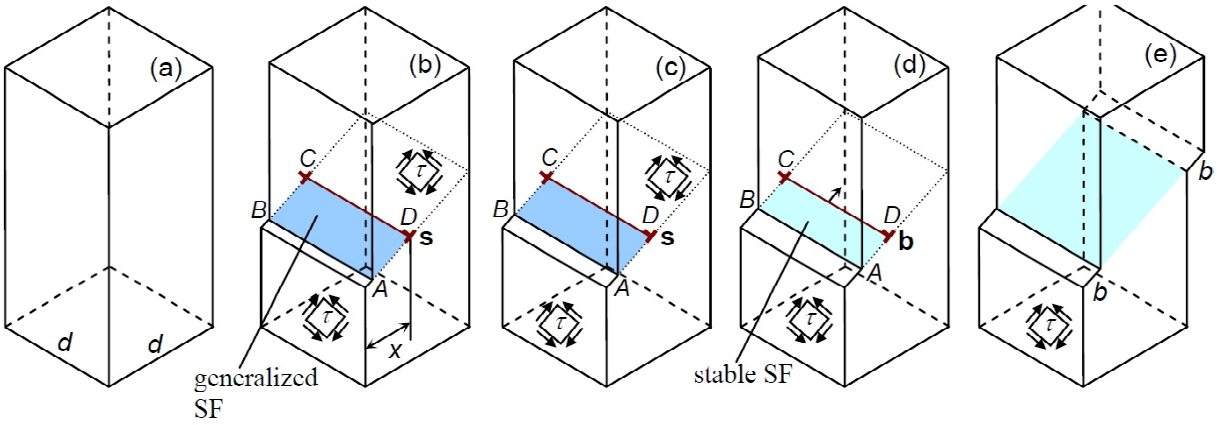

Fig. 1. (Color online) Plastic deformation of a nanowire occurs through generation and evolution of a nanodisturbance. (a) The initial (pre-deformation) state of the nanowire is free from defects. (b) and (c) The nanodisturbance is generated and evolves under the applied shear stress. The Burgers vector magnitude *s* of the non-crystallographic dislocation associated with the nanodisturbance gradually grows, and the generalized stacking fault (ABCD) evolves in parallel with increase in *s*. (d) The nanodisturbance transforms into a conventional partial dislocation when *s* reaches *b*. (e) The geometrically final state of the nanowire contains an isolated stable stacking fault terminated at two free surface steps.

by a 'non-crystallographic' partial edge dislocation CD characterized by a non-quantized ('non-crystallographic') Burgers vector **s** with quite a small magnitude $s < b$, where *b* is the magnitude of the Burgers vector of a conventional 'crystallographic' partial dislocation (Fig. 1b). This defect configuration – the non-crystallographic dislocation and associated generalized stacking fault - is called the near-surface nanodisturbance [11,25].

At the following stage of the nanodisturbance deformation mode, the magnitude *s* continuously increases (Fig. 1c), and the dislocation can move within the nanowire interior. Then, the Burgers vector magnitude *s* of the nanodisturbance reaches the magnitude *b*, in which case the nanodisturbance transforms into a conventional partial dislocation joined by a conventional stable stacking fault (specified by the minimum energy) ABCD with the free surface (Fig. 1d). Finally, the conventional partial dislocation moves and disappears at the free surface (Fig. 1e). As a result, an isolated stacking fault in the nanowire section forms which is terminated at two free surface steps (Fig. 1e).

So, we considered generation and evolution of nanodisturbances in free-standing nanowires under tensile mechanical load. Note that the nanodisturbance deformation mode under consideration can also come into play in nanowires serving as structural elements of bulk nanocomposites containing cracks (Fig. 2). More precisely, when bridging of cracks by nanowires is realized in nanocomposites, these nanowires (as with free-standing nanowires) can be deformed by the nanodisturbance mode (Fig. 2). In doing so, the nanodisturbance deformation mode influences the fracture toughness of bulk nanocomposites containing nanowires as reinforcing inclusions.

3. ENERGY AND STRESS CHARACTERISTICS OF NANODISTURBANCE DEFORMATION MODE IN METALLIC AND COVALENT NANOWIRES AND MICROPILLARS

Let us calculate energy and stress characteristics of the nanodisturbance deformation mode in a nanowire. In doing so, the nanowire is assumed to be an elastically isotropic solid characterized by the shear modulus *G* and the Poisson's ratio ν. In the case under examination, the nanodisturbance deformation mode (Fig. 1) is specified by the following energy change ΔW of the nanowire [11,25]:

$$\Delta W = W_d + W_s + W_\gamma - A, \qquad (1)$$

where W_d is the proper elastic energy of a non-crystallographic dislocation (per its unit length) associated with a nanodisturbance; W_s is the energy of a free surface step related to the generation and evolution of the nanodisturbance; W_γ denotes the energy of the generalized stacking fault; and *A* is the work spent by the shear stress to the generation and evolution of the nanodisturbance.

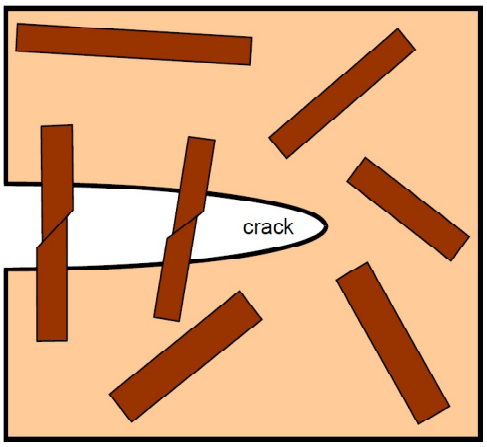

Fig. 2. (Color online) Crack grows in a bulk nanocomposite containing nanowires as reinforcing structural elements. When nanowires provide bridging of cracks, they can be deformed by nanodisturbance mode and thus increase fracture toughness of bulk nanocomposites.

After some algebra presented in Ref. [25], the energy change ΔW is given as follows:

$$\Delta W(x,s) = \frac{Gs^2}{4\pi(1-\nu)}\left(\ln\frac{\min(x,d-x)}{s}+1\right)+\gamma_s s+\gamma_{gsf}(s)\,x/\sqrt{2}-\tau s x/\sqrt{2}. \tag{2}$$

Here s is the Burgers vector magnitude of the non-crystallographic dislocation; x is the distance between the non-crystallographic dislocation core and the free surface connected by the generalized stacking fault with the core; γ_s is the specific energy (per unit area) of the nanowire free surface; and $\gamma_{gsf}(s)$ is the specific energy (per unit area) of the generalized stacking fault, depending on s. In the considered case of metallic and ceramic materials with face-centered cubic lattice (hereinafter called fcc materials), the function $\gamma_{gsf}(s)$ is well approximated by the following analytical expression (see, e.g., [37,38]):

$$\gamma_{gsf}(s/b)=\begin{cases}\dfrac{\gamma_{usf}}{2}\left(1-\cos\dfrac{2\pi s}{b}\right), & 0\le s/b<1/2,\\[2ex] \dfrac{\gamma_{usf}+\gamma_{isf}}{2}-\dfrac{\gamma_{usf}-\gamma_{isf}}{2}\cos\dfrac{2\pi s}{b}, & 1/2\le s/b<1.\end{cases} \tag{3}$$

Here γ_{usf} is the maximum of the function $\gamma_{gsf}(s)$, in which case γ_{usf} characterizes the so-called unstable stacking fault; and γ_{isf} is the energy of the conventional stable stacking fault.

The energy change $\Delta W(x,s)$ (given by formulas (2) and (3)) characterizes generation and evolution of the nanodisturbance. When $s = b$, formula (2) transforms into the standard expression for the energy change specifying generation of a conventional partial dislocation at the nanowire free surface and further glide of the dislocation within the nanowire interior. In this context, formula (2) allows one to calculate the energy characteristics of both the nanodisturbance deformation mode and the classical generation and glide of partial lattice dislocations.

Table 1. Physical parameters of several fcc materials: shear modulus G, Poisson's ratio ν, Burgers vector magnitude b for partial Shockley dislocations, surface energy γ_s, unstable stacking fault energy γ_{usf}, intrinsic stacking fault energy γ_{isf}.

Material	G, GPa	ν	b, nm	γ_s, J/m^2	γ_{usf}, J/m^2	γ_{isf}, J/m^2
Al [39,40]	26	0.35	0.165	1	0.185	0.143
Au [37,39]	27	0.44	0.166	1.48	0.09	0.03
Ni [38,39]	76	0.31	0.144	1.725	0.17	0.12
Pd [40]	44	0.39	0.159	0.684	0.26	0.176
Si [41,42]	64	0.26	0.222	1.2	1.92	0.096
3C-SiC [43,44]	217	0.23	0.178	1.73	2.464	0.08

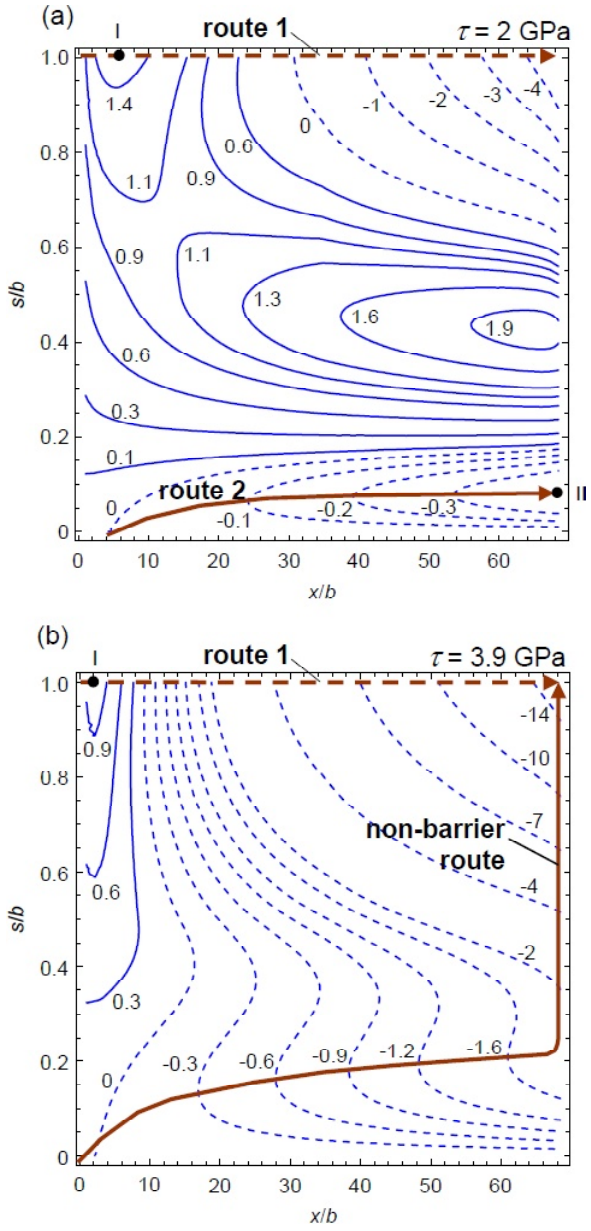

Fig. 3. (Color online) Maps of the energy change $\Delta W(x,s)$ in the case of Ni nanowire with the size d = 10 nm under the external shear stress (a) τ = 2 GPa, and (b) 3.9 GPa. The values of ΔW are given in units of $Gb^2/[2\pi(1-\nu)]$.

With formulas (2) and (3), we calculated the energy change ΔW for several fcc materials: Al (aluminum), Au (gold), Ni (nickel), Pd (palladium), Si (silicon), and 3C-SiC (the cubic phase of silicon carbide). Their parameters exploited in our calculations are presented in Table 1. Fig. 3 shows a typical dependence of the characteristic energy change $\Delta W(x,s)$ as a map in two variables (x,s), calculated for a Ni nanowire with the size d = 10 nm at applied shear stress values of τ = 2 GPa (Fig. 3a) and τ = 3.9 GPa (Fig. 3b). These maps allow one to analyze evolution of the nanowire in the space of variables (x,s) for both the new nanodisturbance deformation mode and the classical glide of partial lattice dislocations.

In the framework of our approach, the final state of the nanowire (the state with an isolated stacking fault terminated at two free surface steps (Fig. 1e) which is formed after one elementary act of plastic deformation) is specified by the coordinates (x=d-b, s=b) in the map and corresponds to the upper right corner of the map (Fig. 3). The classical generation and glide of a partial lattice dislocation is characterized by the dashed line with head arrow (route 1) in Fig. 3. The classical deformation is specified by an energy barrier (at point I) which is weakly sensitive to the applied stress, because the barrier value is mostly related to the generation of a free surface step during the generation of a dislocation. In these circumstances, the classical deformation mode can be realized as only a thermally activated process and cannot occur at temperature T= 0K. At the same time, in the absence of thermal fluctuations at T = 0K, the nanodisturbance deformation mode (see solid route 2 in Fig. 3) can operate in nanowires and micropillars. For a comparatively low level of the applied stress (Fig. 3a), a nanodisturbance in a nanowire is generated, but its evolution is not complete in the sense that the nanowire with the nanodisturbance reaches some intermediate state (point II in Fig. 3a) having the minimum energy, which is different from the geometrically final state (corresponding to formation of an isolated stable stacking fault terminated by free surface steps; see Fig. 1e) characterized by x=d-b and s=b. When the external stress reaches its critical value τ_c, the nanowire evolves into its geometrically final state (x=d-b, s=b) in the athermal, non-barrier way (Fig. 3b). Thus, the nanowire at temperature T = 0K can be deformed by only the nanodisturbance mode (but not the classical dislocation glide), if the applied stress reaches its critical value τ_c.

We calculated the critical shear stress τ_c (the minimum stress at which the nanodisturbance deformation mode occurs in the athermal way in the nanowire and results in its geometrically final state) as a function of the nanowire/micropillar size d ranging from 1 to 500 nm, for several fcc materials (Fig. 4). Figs. 4a and 4b present the calculated dependences $\tau_c(d)$, for metals (Al, Au, Ni, Pd) and covalent materials (Si, 3C-SiC), respectively. The dependences show that the nanodisturbance deformation mode in metallic nanowires/micropillars is typically characterized by the critical shear stress $\tau_c \sim G/10$ (Fig. 4a). These values of τ_c are of the same order

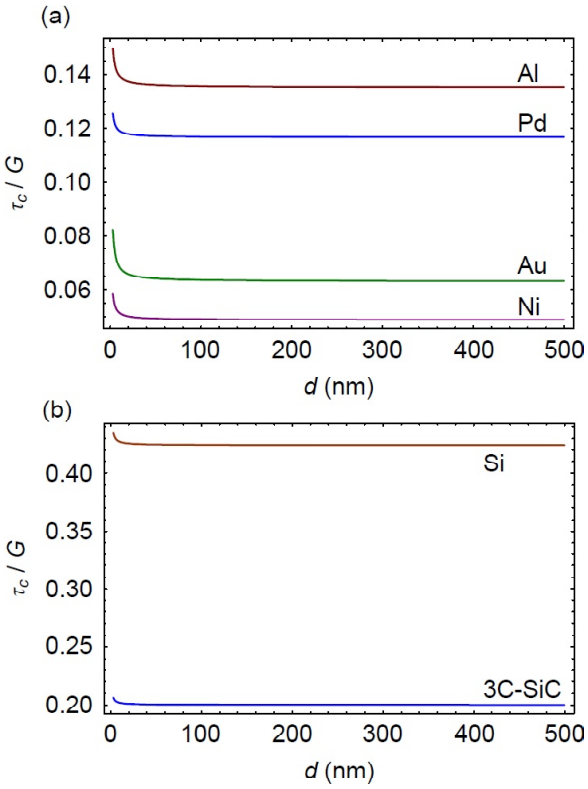

Fig. 4. (Color online) Dependence of the critical stress τ_c (the smallest stress at which the nanodisturbance deformation mode occurs in the non-barrier way) on the nanowire size d in (a) fcc metal nanowires: Al, Au, Ni and Pd; and (b) covalent nanowires: Si and 3C-SiC.

as the ultimate stresses experimentally measured [4,6,7,9,10,12-15,18] in metallic micropillars. In covalent fcc materials, values of the critical shear stress $\tau_c > G/5$ (Fig. 4b), first of all, due to extra high energy of the generalized stacking fault (see values of the unstable stacking fault energy γ_{usf} in Table 1). With these values of τ_c, the nanodisturbance deformation mode hardly occurs in nanowires/micropillars made of such covalent materials as Si and 3C-SiC. In addition, generally speaking, the dependences $\tau_c(d)$ (Fig. 4) are indicative of the trend that the strength of nanowires and micropillars increases with decreasing their characteristic size d.

4. CONCLUDING REMARKS

Thus, the nanodisturbance deformation mode can effectively occur at very high applied stresses and temperature $T = 0$K in such metallic nanostructures as free-standing metallic nanowires, micropillars and nanowires serving as structural elements of bulk nanocomposites. In doing so, in examined cases of typical fcc metals (Al, Au, Ni, Pd) with low, intermediate and large energies of the stacking fault, the nanodisturbance deformation mode in metallic nanowires/micropillars is characterized by the critical shear stress $\tau_c \sim G/10$ (Fig. 4a). These values of τ_c are extremely high; they are close to the theoretical strength and are of the same order as the ultimate stresses experimentally measured [4,6,7,9,10,12-15,18] in metallic micropillars. In such covalent fcc materials as Si and 3C-SiC, values of the critical shear stress $\tau_c > G/5$ (Fig. 4b), first of all, due to extra high energy γ_{usf} of the unstable stacking fault energy (see Table 1). With these values of τ_c, the nanodisturbance deformation mode at temperature $T = 0$K hardly occurs in nanowires/micropillars made of Si and 3C-SiC. At the same time, when temperature is high enough, thermal fluctuations are capable of enhancing operation of the nanodisturbance deformation mode which, in any event, is more energetically favorable than the classical dislocation glide.

Also, the dependences $\tau_c(d)$ (Fig. 4) for both metallic and covalent fcc materials are indicative of the trend that the strength of nanowires and micropillars increases with decreasing their characteristic size d. For $d > 100$ nm, the strength is weakly sensitive to the nanowire/micropillar size d.

ACKNOWLEDGEMENTS

This work was supported, in part, (for S.V.B.) by the Russian Ministry of Education and Science (Grant 14.B25.31.0017), and (for I.A.O.) by St. Petersburg State University research grant 6.37.671.2013.

REFERENCES

[1] J. Bürki, R.E. Goldstein and C.A. Stafford // *Phys. Rev. Lett.* **91** (2003) 254501.
[2] M.Yu. Gutkin, I.A. Ovid'ko and A.G. Sheinerman // *J. Phys.: Condens. Matter* **15** (2003) 3539.
[3] I.A. Ovid'ko and A.G. Sheinerman // *Philos. Mag.* **84** (2004) 2103.
[4] M.D. Uchic, D.M. Dimiduk, J.N. Florando and W.D. Nix // *Science* **305** (2004) 986.
[5] T. Kizuka, Y. Takatani, K. Asaka and R. Yoshizaki // *Phys. Rev. B* **72** (2005) 035333.
[6] J.R. Greer and W.D. Nix // Phys. Rev. B **73** (2006) 245410.
[7] J.R. Greer // *Rev. Adv. Mater. Sci.* **13** (2006) 59.
[8] I.A. Ovid'ko and A.G. Sheinerman // *Adv. Phys.* **55** (2006) 627.
[9] S. Brinckmann, Ju-Young Kim and J.R. Greer // *Phys. Rev. Lett.* **100** (2008) 155502.

[10] S.H. Oh, M. Legros, D. Kiener and G. Dehm // *Nature Mater.* **8** (2009) 95.
[11] S.V. Bobylev and I. A. Ovid'ko // *Phys. Rev. Lett.* **103** (2009) 135501.
[12] A.T. Jennings, M.J. Burek and J.R. Greer // *Phys. Rev. Lett.* **104** (2010) 135503.
[13] Q. Yu, Z.-W. Shan, J. Li, X. Huang, L. Xiao, J. Sun and E. Ma // *Nature* 463 (2010) 335.
[14] J.R. Greer and J.T.M. De Hosson // *Progr. Mater. Sci.* **56** (2011) 654.
[15] D. Jang and J.R. Greer // *Scr. Mater.* **64** (2011) 77.
[16] M.J. Lagos, F. Sato, D.S. Galvão and D. Ugarte // *Phys. Rev. Lett.* **106** (2011) 055501.
[17] I.A. Ovid'ko // Appl. Phys. Lett. **99** (2011) 061907.
[18] N.Q. Chinh, T. Gyori, R.Z. Valiev, P. Szommer, G. Varga, K. Havancsak and T.G. Langdon // *MRS Commun.* **2** (2012) 75.
[19] S.V. Bobylev and I.A. Ovid'ko // *Phys. Rev. Lett.* **109** (2012) 175501.
[20] S.V. Bobylev and I.A. Ovid'ko // *Rev. Adv. Mater. Sci.* **35** (2013) 25.
[21] K.A. Bukreeva, R.I. Babicheva, S.V. Dmitriev, K. Zhou and R.R. Mulyukov // *JETP Lett.* **98** (2013) 91.
[22] E. Rabkin and D.J. Srolovitz // *Nano Lett.* **7** (2007) 101.
[23] T.Zhu, J. Li, A. Samanta, A. Leach and K. Gall // *Phys. Rev. Lett.* **100** (2008) 025502.
[24] A. Cao and Y. Wei // *Phys. Rev. B* **74** (2006) 214108.
[25] S.V. Bobylev and I.A. Ovid'ko // *Phys. Rev. B* **84** (2011) 054111.
[26] X. Han, K. Zheng, Y.F. Zhang, X. Zhang, Z. Zhang and Z.L. Wang // *Adv. Mater.* **19** (2007) 2112.
[27] H. Ikeda, Y. Qi, T. Cagin, K. Samwer, W.L. Johnson and W.A. Goddard III // *Phys. Rev. Lett.* **82** (1999) 2900.
[28] P.S. Branicio and J.P. Rino // *Phys. Rev. B* **62** (2000) 16950.
[29] I.A. Ovid'ko // Scr. Mater. **66** (2012) 402.
[30] M.Yu Gutkin, T. Ishizaki, S. Kuramoto and I.A. Ovid'ko // *Acta Mater.* **54** (2006) 2489.
[31] M.Yu. Gutkin and I.A. Ovid'ko // *Appl. Phys. Lett.* **88** (2006) 211901.
[32] M.Yu Gutkin and I.A. Ovid'ko // *Acta Mater.* **56** (2008) 1642.
[33] I.A. Ovid'ko and A.G. Sheinerman // *J. Phys.: Condens. Matter*. **18** (2006) L225.
[34] J.P. Cui, Y.L. Hao, S.J. Li, M.L. Sui, D.X. Li and R. Yang // *Phys. Rev. Lett.* **102** (2009) 045503.
[35] N. Bernstein and E.B. Tadmor // *Phys. Rev. B* **69** (2004) 094116.
[36] P. Lazar and R. Podloucky // *Phys. Rev. B* **75** (2007) 024112.
[37] H.S. Park and J.A. Zimmerman // *Phys. Rev. B* **72** (2005) 054106.
[38] X.-L. Wu, Y.T. Zhu and E. Ma // *Appl. Phys. Lett.* **88** (2006) 121905.
[39] J.P. Hirth and J. Lothe, *Theory of Dislocations* (New York: Wiley, 1982).
[40] J. Hartford, B. von Sydow and G. Wahnström // *Phys. Rev. B* **58** (1998) 2487.
[41] R.J. Jaccodine // *J. Electrochem. Soc.* **110** (1963) 524.
[42] B. Joós, Q. Ren and M.S. Duesbery // *Phys. Rev. B* **50** (1994) 5890.
[43] Z. Ding, S. Zhou and Y. Zhao // *Phys. Rev. B* **70** (2004) 184117.
[44] P. Vashishta, R.K. Kalia, A. Nakano and J.P. Rino // *J. Appl. Phys.* **101** (2007) 103515.